HiSST: 2nd International Conference on
High-Speed Vehicle Science & Technology
11–15 September 2022, Bruges, Belgium

HEXAFLY-INT: An Overview of Waverider Subsonic Investigations

Tamas Bykerk[1], Jonathan Jeyaratnam[2], Dries Verstraete[2], Johan Steelant[3]

Abstract

Hypersonic waveriders have the potential to significantly reduce travel times on long haul civilian transport routes. The design of hypersonic aircraft is heavily influenced by the aerodynamic efficiency at the cruise Mach number, resulting in less than ideal geometries for subsonic flight. Waverider aerodynamics and stability in the low speed regime is rarely investigated and not well understood, but is crucial for horizontal take-offs and landings. This paper gives an overview of all work completed within the HEXAFLY-INT project with respect to subsonic investigations. It covers a wide range of static and dynamic wind tunnel tests in the longitudinal and lateral-directional planes. The experimental investigations are complemented by in depth numerical computations which validate the experimental data. It was found that flow separation, non-linear vortex lift and subsequent bursting at high angles of attack govern the aircraft stability derivaties. This is due to the low aspect ratio, highly swept delta wings which are present on the vehicle, as well as sharp edges which give rise to high pressure gradients at moderate angles of attack.

Keywords: *Hypersonic, Waverider, Stability, Wind Tunnel, CFD*

Nomenclature

Latin
AoA – Angle of Attack
AoS – Angle of Sideslip
CFD – Computational Fluid Dynamics
CoG – Centre of gravity
EDF – Electric ducted fan
$EFTV$ – Experimental flight test vehicle
LSV – Low speed variant
UDF – User defined function
WT – Wind Tunnel
Greek
α – Angle of Attack
β – Angle of Sideslip
δ – Control surface deflection
Subscripts
D – Drag force
e – Elevon
l – Roll moment
L – Lift force
m – Pitch moment
n – Yaw moment
p – Roll rate
q – Pitch rate
r – Yaw rate
r – Rudder
Y – Side force

1. Introduction

In the early 20th century, aerospace research was dominated by the quest for higher speeds. This culminated in manned hypersonic flight between 1958 and 1968 with the X-15 program, where a selected group of pilots flew in excess of Mach 6. Since then, piloted vehicles reaching these speeds have been limited to spacecraft during the launch and re-entry phases of flight.

[1] *The German Aerospace Center (DLR), Bunsenstr. 10, Göttingen, Lower Saxony, 37073, Germany, tamas.bykerk@dlr.de*
[2] *School of Aerospace, Mechanical and Mechatronic Engineering, Faculty of Engineering, The University of Sydney, NSW, 2006, Australia, dries.verstraete@sydney.edu.au*
[3] *ESA-ESTEC, Flight Vehicles and Aerothermodynamics Engineering Section, Noordwijk, The Netherlands, johan.steelant@esa.int*

History shows that commercial high speed vehicles are rarely taken past the concept phase, as they are limited by low cruise efficiency, high fuel consumption and reduced range [1]. Some success in the supersonic civil market was found between 1979 and 2003 with the Concorde. However, high seat-per-mile costs as well as strong resistance from environmental and political groups due to noise, emissions and the sonic boom ultimately resulted in its downfall [2]. For this reason the commercial aviation sector has maintained focus on aircraft with modest transonic cruise speeds and high fuel efficiency, providing the possibility of direct flights between almost any global city pair. If current trends continue, ultra long-haul flights will begin exceeding 20 hours, which can have negative physical effects on both passengers and crew. Industry has recognised this and is performing research with ultra long-haul test flights, such as those carried out by Qantas within "Project Sunrise". On the 20th of October 2019, a commercial airliner spent a record 19 hours and 16 minutes in the air from New York to Sydney. The effects of ultra-long-haul flights on crew fatigue and passenger jetlag were assessed during the flight, with tests ranging from monitoring pilot brain waves, melatonin levels and alertness, to exercise classes for passengers [3]. While this investigation will prove useful for regulators and airlines which impose strict duty times, the reduction in flight duration achieved by hypersonic flight eliminates these issues. Therefore, flights of this range would become more attractive if the duration was reduced to four hours or less [4].

Recently, radically new hypersonic waverider concepts integrating highly efficient air breathing engines are challenging the need for ultra long-haul flights [5, 6, 7]. Advances in propulsion technology and waverider design methodologies creating high lift-to-drag ratios are showing potential to solve the problems which have previously hampered progress. To combat sonic boom issues, routes such as Brussels to Sydney would fly over the north pole and the pacific ocean to maximise high speed cruise. Table 1 [8] shows a comparison of current and potential flight times for a new Mach 8 waverider vehicle concept.

Table 1. Current versus potential flight times for a Mach 8 vehicle (*indirect flight) [8]

Route	Current	Potential
Brussels - Sydney	21h 55m*	2h 47m
Brussels - Los Angeles	10h 30m	2h 20m
Brussels - Tokyo	10h 40m	2h 13m

Waveriders achieve high aerodynamic efficiency at cruise as the body shock is contained by the wing leading edges, allowing the vehicle to ride its own shockwave. This design requires a sharp and slender vehicle with highly swept, low aspect ratio wings. To contain the shockwave, low mounted wings with anhedral are often implemented despite the known adverse effect on low speed lateral stability [9]. This is governed by the high speed design point requirements and cannot be avoided. The overwhelming bulk of waverider research is focused on areas such as aerodynamic design [10, 11, 12, 13], aero-thermodynamics [14, 15], propulsion systems [16, 17, 18] and flight dynamics [19, 20, 21, 22] for the cruise Mach number, while the critical low speed phases are typically ignored.

Besides the work presented in this paper, two main studies looked briefly into the low speed handling qualities of hypersonic vehicles. The LoFLYTE project complemented wind tunnel (WT) tests with a subsonic flight test program. While successful flight tests inherently indicate that the vehicle was both statically and dynamically stable, the dynamic derivatives were never presented [23, 24, 25, 26, 27, 28, 29]. Similarly, low speed flight tests of the X-43A-LS vehicle never quantified any stability derivatives [30, 31]. In addition, the wing and control surfaces for the low speed experiments were enlarged considerably which prevented a true understanding of the subsonic behaviour of the high speed design.

Looking to the future, the HEXAFLY-INT project aims to facilitate the flight testing of several break-through technologies at high speed [32, 33]. This will create the groundwork to gradually increase the technology readiness level until passenger services are introduced. Under HEXAFLY-INT, two distinctly different flight tests are considered. The hypersonic experimental flight test vehicle (EFTV) is for testing

the high-speed cruise performance of a non-propelled glider. It will be launched by the Brazilian VS50 sounding rocket with an 8-ton solid rocket motor in a suborbital trajectory having an apogee at about 100 km. In this experimental phase, the EFTV aims to demonstrate a high aerodynamic efficiency (L/D $\geq$ 4), a positive aerodynamic balance at controlled cruise Mach numbers (7 - 8) and an optimal use of advanced high-temperature materials and structures. The trajectory of the flight is shown in Figure 1 (a), while the vehicle is presented in Figure 1 (b).

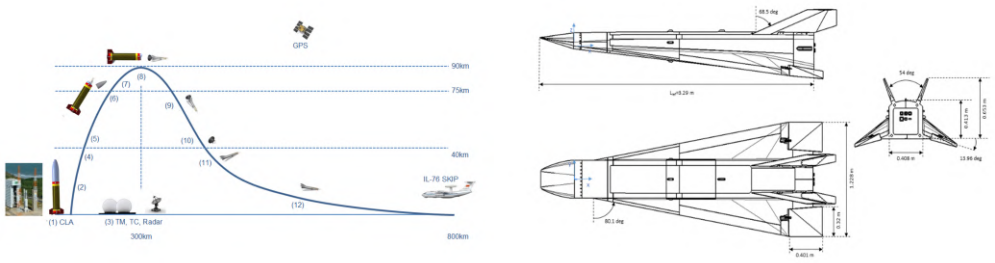

(a) **(b)**

Fig 1. (a) Flight path of the EFTV and (b) 3 view drawing of the EFTV

Besides the high-speed flight test, an additional low-speed flight experiment will be performed to cross-check the viability of the vehicle concept for later deployment as a passenger aircraft. It entails a flight experiment of the low speed variant (LSV), a scaled, remotely piloted vehicle at the University of Sydney Marulan flight test facility to verify take-off and landing, as well as low subsonic cruise and handling qualities. Similar to the LoFLYTE and X-43A programs, the LSV will be fitted with an electric ducted fan (EDF) to fly under its own power. To support the low speed flight test campaign, a complete aerodynamic database is required to ensure controllability and flyability.

This paper collates selected results from all subsonic static and dynamic results completed at the University of Sydney within the framework of the HEXAFLY-INT project [34, 35, 36, 37, 38, 39, 40, 41]. The following section explains the various methodologies used for CFD and WT experiments. The results and discussion will evaluate the data presented before the summary of findings.

2. Methodology

2.1. CFD

Static simulations of the glider and LSV were completed using similar unstructured meshes with a coarse bullet shaped farfield and a body of influence around the vehicle for volumetric refinement. The boundaries extended 20 vehicle's reference lengths upstream and 30 downstream. Fifteen prism inflation layers around the vehicle were sized to have a wall y^+ of 1. For longitudinal computations, a half domain with a symmetry condition was used to save on cell count and computation time. For lateral-directional cases, or those with asymmetric control deflections, a full grid was used. Figure 2 shows an example the mesh domain with a close up of the aircraft surface mesh.

The farfield was composed of a velocity inlet with a pressure outlet at the discharge. Standard sea level conditions were used at the boundaries. The steady state, pressure based, coupled solver in ANSYS Fluent was used along with the k-ω-SST turbulence model and second order spatial discretisation. The pressure based solver was selected because the flow at 20 m/s is considered incompressible and it does not suffer from numerical stiffness seen in density based solvers. Turbulence intensity levels were taken from WT characterisation tests to provide comparable test conditions.

For dynamic simulations the forced oscillation technique was used. The same meshes from the static simulations were used for the dynamic cases, where a deforming mesh or a rotation interface was used. This technique required the use of the pressure based Unsteady Reynolds Averaged Navier Stokes (URANS) solver from ANSYS Fluent. For consistency, the k-ω-SST turbulence model was retained from

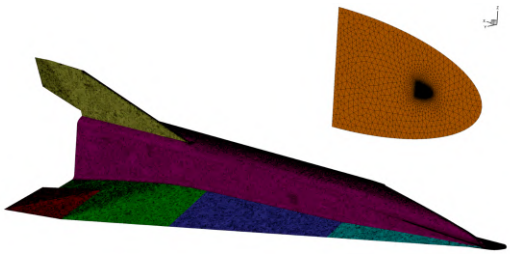

Fig 2. Close up of CFD surface mesh and farfield

the static computations. The vehicle motion was achieved using a user defined function (UDF) for each movement profile. A range of frequencies between 0.5 and 2 Hz with varying amplitudes up to 4 degrees were investigated. The frequencies and amplitudes were selected based on the consideration of values used for similar investigations [42, 43, 44, 45, 46, 47, 48].

2.2. Wind Tunnel Tests

WT experiments were conducted in two facilities (The University of Sydney 7 foot $\times$ 5 foot and 3 foot $\times$ 4 foot test sections). Examples of the different models developed over the years are presented in Figure 3.

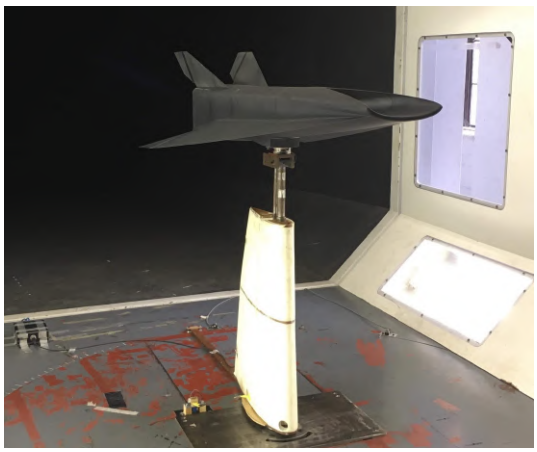

(a)

(b)

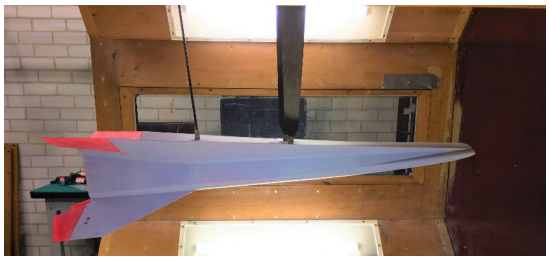

(c)

(d)

Fig 3. WT models spanning 2017 to 2020 showing (a) LSV with internal fan, (b) glider used for initial static tests, (c) LSV without internal fan and (d) glider used for dynamic tests

Early models such as that seen in Figure 3 (b) were constructed using layers of milled wood, while later models seen in Figure 3 (a) and (c) were constructed completely of 3D printed plastic. The model

presented in Figure 3 (a) was used to better understand the flow conditions through the modified scramjet duct. Static pressure measurements were taken upstream and downstream of the fan (Figure 4 (a)), while total measurements were recorded at the fan face using the rake shown in Figure 4 (b).

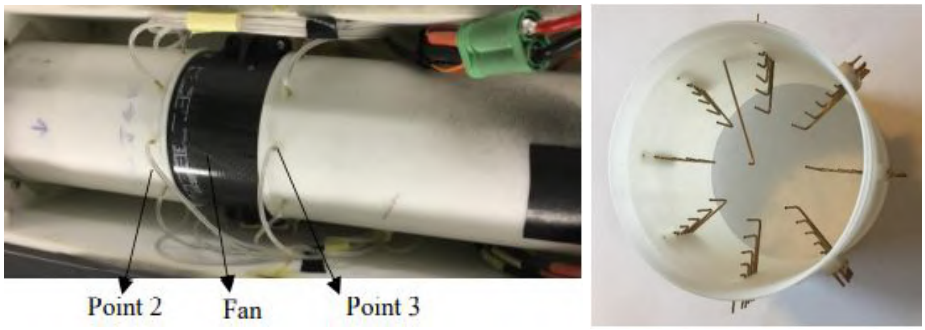

(a) **(b)**

Fig 4. (a) Static wall taps up-and-downstream of the fan for pressure jump specification and (b) Total pressure rake with static wall taps for flow quality analysis

Static tests were conducted using fixed attachments to either a 6 component load cell or overhead load balance. Ange of attack (AoA) and Angle of Sideslip (AoS) sweeps were conducted with force and moment measurements recorded for each angle setting. For dynamic testing, measurements were taken using UAVMainframe, a system developed by Lehmkueler [49], and further developed by Anderson [50]. It is a sophisticated real time flight control and data acquisition system. It is capable of providing an interface with ground control software to control flight tests whilst obtaining high quality synchronised data from many sensors, fusing the resulting data and providing highly accurate data for immediate real time use by the flight controller, and for post flight analysis and system identification routines. The model used for dynamic testing shown in Figure 3 (d) was attached to a single axis gimbal (free to rotate in pitch), with active control surfaces peturbing the vehicle from a trimmed flight condition in the WT. Counterbalance weights were used to shift the center of gravity forward to the desired location. A view of the internal layout of the model used for dynamic testing is shown in Figure 5.

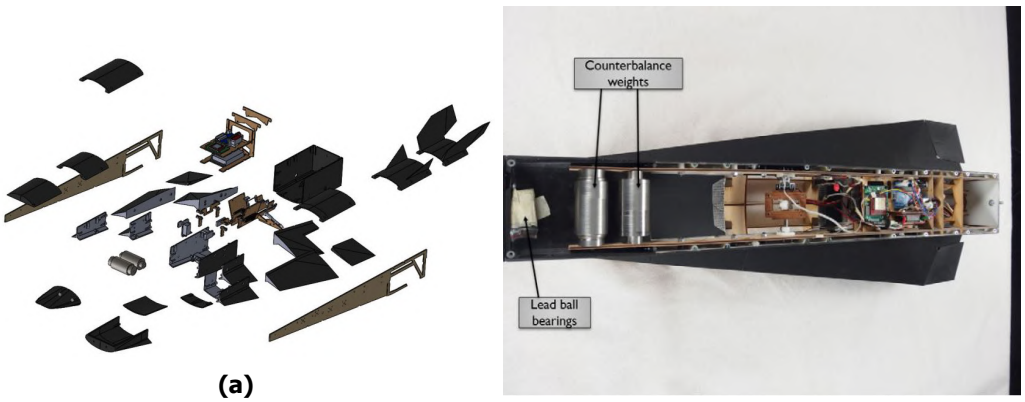

(a) **(b)**

Fig 5. (a) Exploded view of complete CAD model (fasteners hidden for clarity) and (b) Model showing fully installed internal components

2.3. Test Summary

Figure 6 presents the standard axis convention in the body and stability reference frames about the centre of gravity (CoG). Multiple CoG locations have been investigated throughout the various test campaigns. Where moment results are presented in the results section, the CoG locations are specified. The location of the origins for the glider and LSV are given in Figure 7.

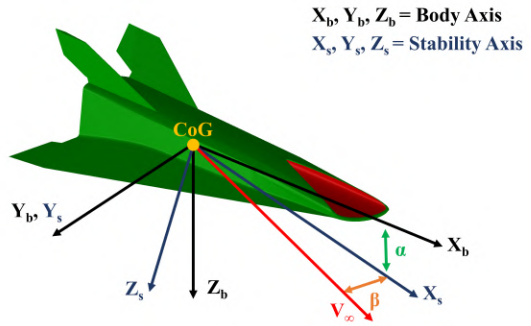

Fig 6. Axes definitions

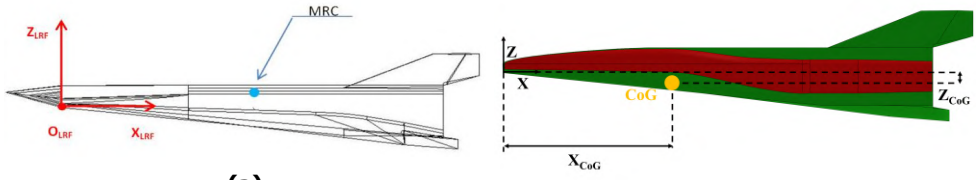

(a) **(b)**

Fig 7. CoG definitions for (a) glider and (b) LSV

A summary of completed tests are presented in Table 2. Static AoA sweeps were typically conducted between -5 and 25 degrees. Static AoS sweeps were performed between -10 and 10 degrees at set AoA between -5 and 15 degrees AoA with 5 degree increments.

Table 2. Summary of completed tests for WT-LSV(1), CFD-LSV(2), WT-Glider (3) and CFD-Glider (4) (*limited AoA sweep, **AoS variation at selected AoA and 0 AoS)

Test	Clean	δ_e	δ_a	δ_r	Press. Taps	Flow Vis.
Static AoA sweep	1,2,3,4	1,2,3,4	1,2	1,2		1,3
Static AoS sweep	1,2,3,4		1,2	1,2		
Active Fan	1,2				1	
Dynamic AoA sweep	2*,3,4					
Dynamic AoS sweep	2**					
Dynamic plunge	2*					
Dynamic side-to-side slip	2**					

Pressure tapped tests were only conducted with the active fan as the pressure taps were located inside the duct to characterise static conditions upstream and downstream of the fan. These were used as boundary conditions for the CFD reconstruction of the tests. Flow visualisation tests were used

for indentifying vortex structures at the wing leading edges. Dynamic sweeps relate to the AoA or AoS oscillation about a selected AoA. Plunge relates to the AoA inducing vertical translation of the vehicle, while side-to-side slip is a motion which induces AoS through translation along the y-axis of the vehicle.

3. Results and Discussion

This section will present a short overview of selected results from the numerical and experimental investigations completed.

Figure 8 shows a comparison of WT results for lift, drag, pitching moment, and lift-to-drag ratio at the 44.4% CoG location. Excellent agreement between both datasets is observed, with the exception of AoAs above 15 degrees, where a maximum deviation of 10% in pitching moment is seen. A maximum lift-to-drag ratio of approximately 3.7 at 5 degrees AoA is significantly lower than typical subsonic aircraft, but this is expected given the vehicle shape and planform [9]. It is predicted that the L/D would improve with a full scale vehicle (approximately 90 metres long) due to lower drag from increased Reynolds number.

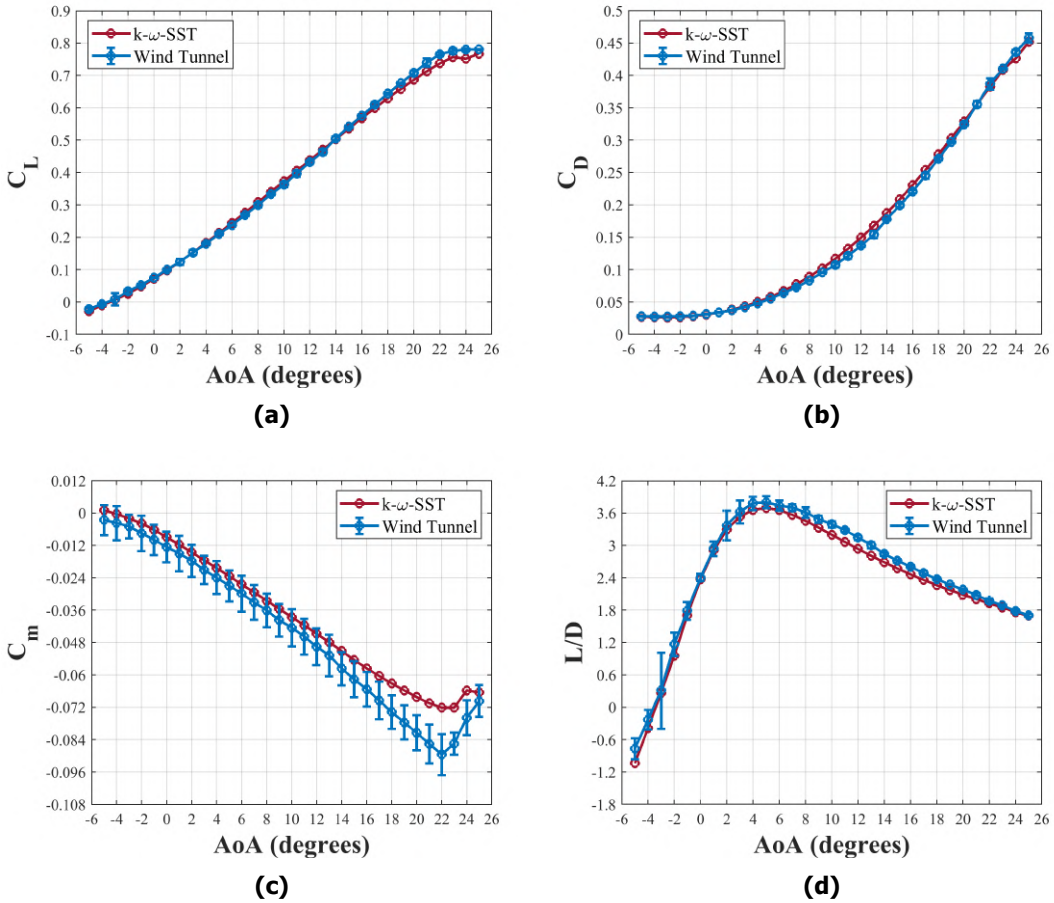

Fig 8. Comparison of CFD and WT coefficients for an angle of attack sweep showing (a) lift, (b) drag, (c) pitching moment and (d) lift-to-drag ratio

The lift curve slope is non-linear as the sharp, highly swept wing geometry promotes leading edge flow separation and subsequent formation of vortices. The growth of these vortices with increasing AoA is illustrated using post processed CFD images in Figure 9. Complex vortex structures are observed,

with 3 main regions of vorticity along the wing. Additionally, vortices form along the fuselage wall and at the upper inlet lips at high AoA. No clear stall point was found, but a levelling off in lift coefficient was seen at approximately 22 degrees AoA. This also coincides with a sharp gradient change in the pitching moment plot which was picked up in both the CFD and WT datasets despite the disagreement in magnitudes. This is explained by vortex breakdown and bursting as observed when comparing Figure 9 (c) and Figure 9 (d). The vorticity magnitude in 9 (d) for the aft slices of the wing is clearly diminished. Lateral-directional simulations also highlighted the importance of understanding the vortex systems. As seen in Figure 10, multiple vortices are present on the leeward sides of the fins and make non-linear contributions to the generated sideforce with increasing AoS.

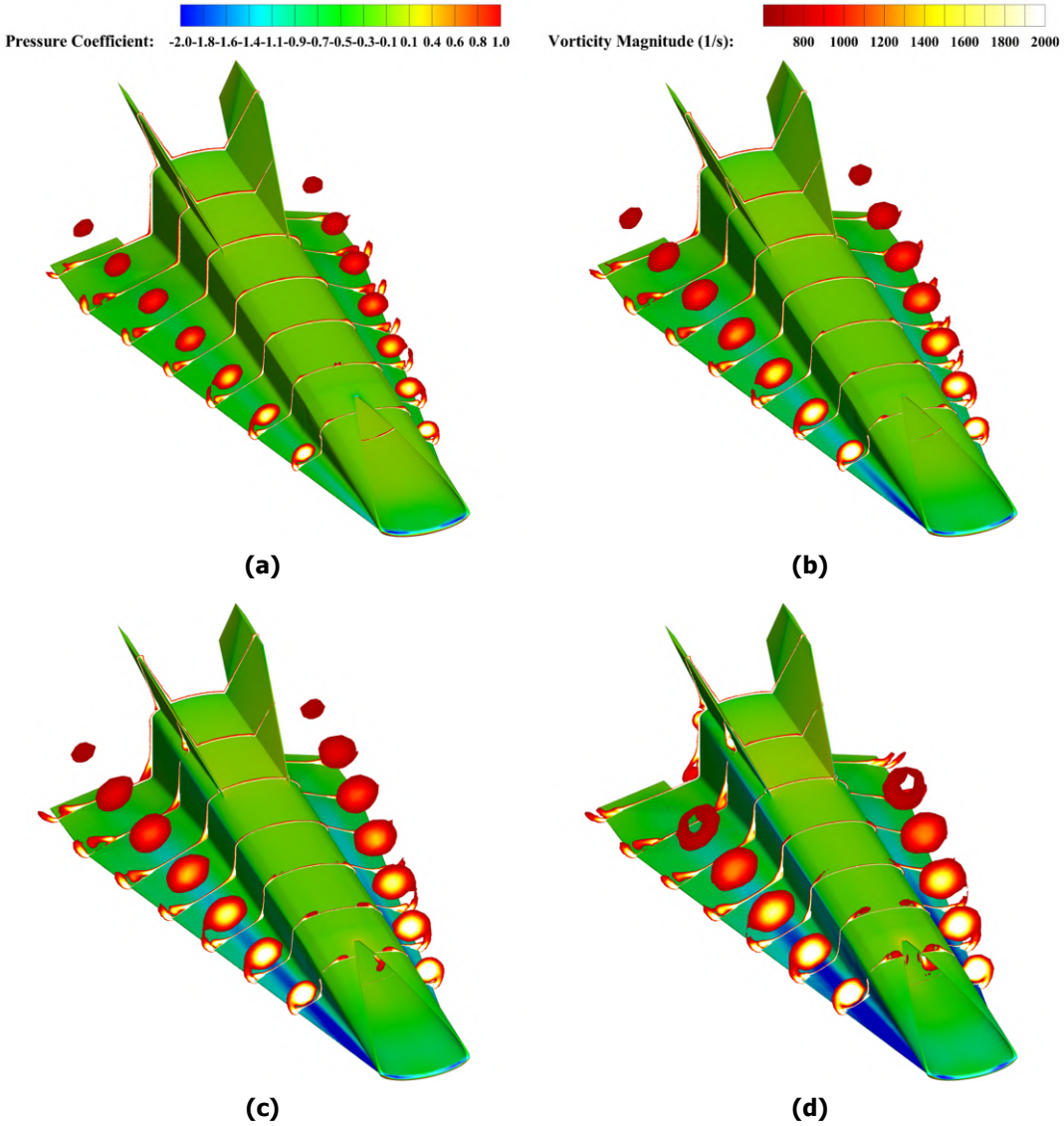

Fig 9. CFD images showing vortex development through angle of attack range (a) 10 degrees, (b) 15 degrees, (c) 20 degrees and (d) 25 degrees

Results presented in Figure 11 show a comparison between CFD and WT experiments conducted with the glider for static and dynamic derivatives at a moment reference center at 38%. Dynamic CFD data is from an excitation frequency of 1Hz and both 1 and 4 degrees AoA amplitude. Overall the correlation between all datasets is high despite the CFD computations using a different methodology to calculate

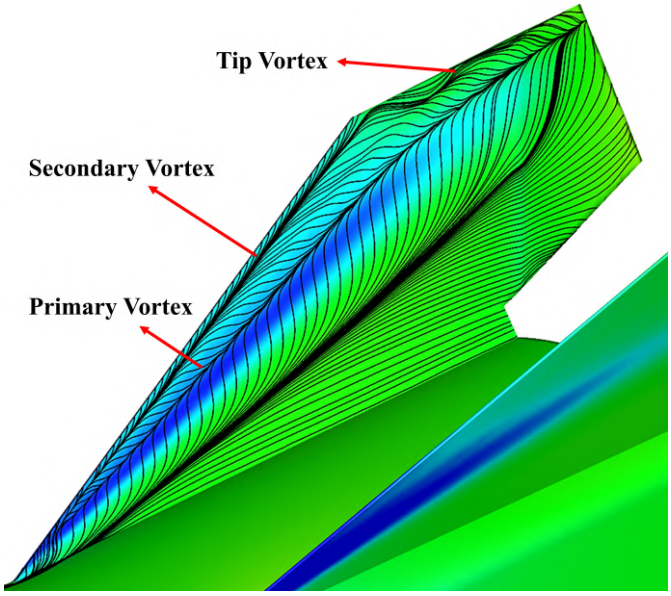

Fig 10. Sideslip induced vortex development on fins at 15 degrees AoA and 8 degrees AoS

the derivatives to the WT (forced oscillation vs. free to pitch).

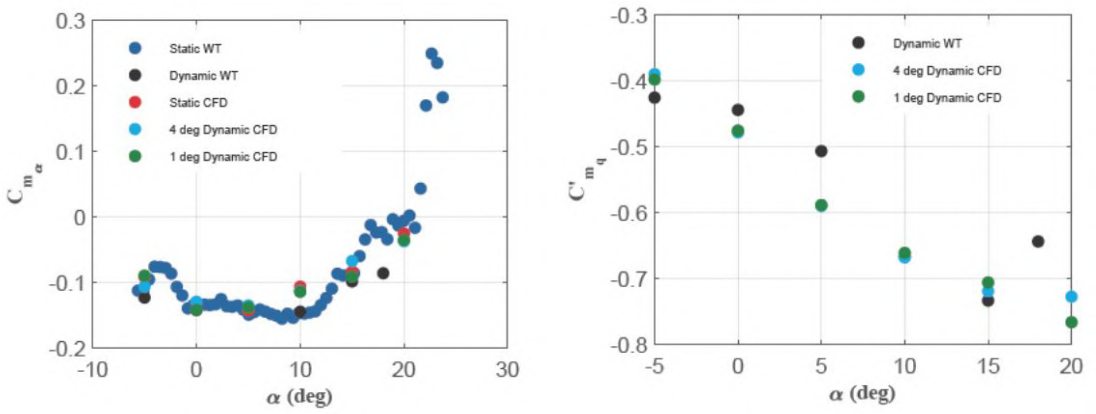

(a) **(b)**

Fig 11. Comparison between CFD and WT derived pitch derivatives for glider configuration showing (a) pitch stiffness and (b) pitch damping

Figure 12 (a) shows an example of the hysteresis loops from yawing simulations for the LSV at 0 degrees AoA alongside the derivatives for the full AoA range. Sideforce and yawing moment results show damping behaviour, but rolling moment appears to be susceptible to instabilities over the entire AoA range. However, as this is the combined derivative it is unclear as to whether this is due to the side slip or the yawing motion. With increasing AoA the side force is observed to drop slightly which is caused by the fuselage restricting flow to the fins and impeding their effectiveness. This is accompanied by a similar trend in the yawing moment derivative, which is expected as the fin side force is a main contributor to the yawing moment. Overlaid static from steady-state CFD simulations shows good correlation with the points of no rate in the dynamic motion. This shows that there are no large dynamic effects present.

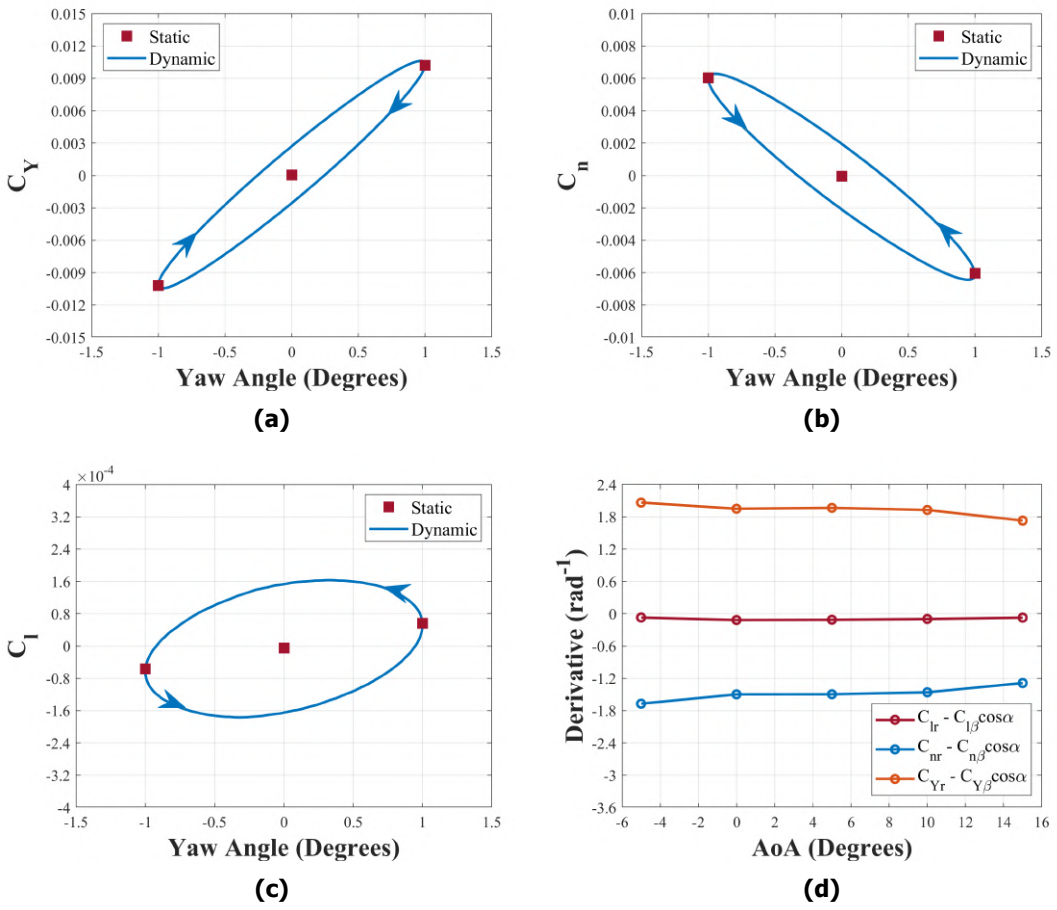

Fig 12. Examples of hysteresis loops for the yawing case showing coefficients of (a) side force AoA (b) yawing moment (c) rolling moment and (d) The calculated combined yawing and sideslip derivatives over the AoA range

Contour plots of x-velocity at various duct locations are shown in Figure 13 for the anticipated take-off, cruise and landing throttle settings and AoA. All flight conditions show a similar flowfield, which is dominated by dual vortices originating at the inlet lip. The areas in red highlight low x-velocity and show the location of the vortex cores which appear to grow in size as they propagate through the duct, particularly after passing the S-bend. While the upper lips have been rounded slightly, they are extremely thin and the flow is not able to remain attached as it is ingested by the intake. The vortices appear to gravitate towards the lower section of the duct where the S-bend transition starts to occur. No separation due to adverse pressure gradients at the duct bend is observed. This is attributed to the low bend radius of the geometry combined with the suction provided by the fan. These vortices are present during each phase of flight analysed and cause significant intake distortion.

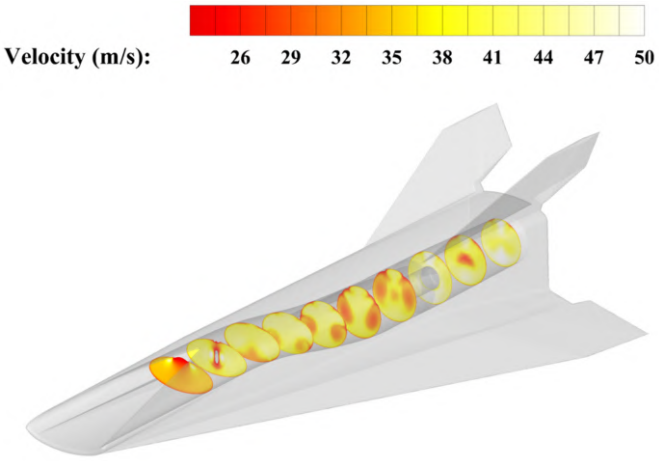

(a)

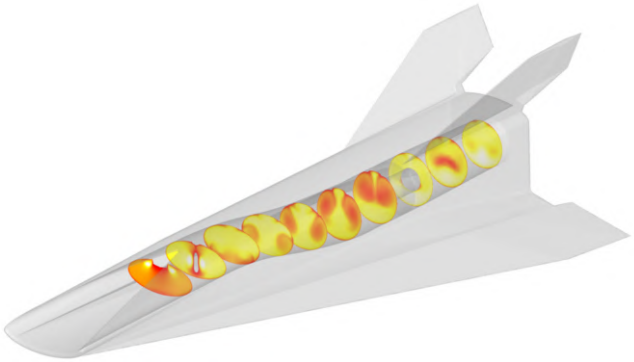

(b)

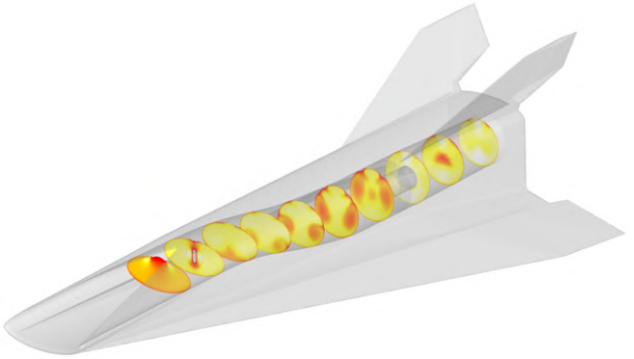

(c)

Fig 13. CFD images showing vortex progression through duct at conditions indicative of (a) take-off (20 A, 15 m/s and 10 degrees AoA), (b) landing (10 A, 15 m/s and 10 degrees AoA) and (c) cruise (20 A, 20 m/s and 5 degrees AoA)

The work presented here is highly specific to the LSV, but the flow features identified do have relevance for a full scale configuration such as the LAPCAT II MR2 concept. This vehicle uses a secondary duct system for the low speed propulsion systems, with the air needing to come through parts of the high speed inlet. The sharp edges of the lips make the low speed propulsion systems susceptible to vortex ingestion. The results from CFD were validated in the WT, with an example of total pressure contours at the fan face showing strong agreement between CFD and experimental results shown in Figure 14.

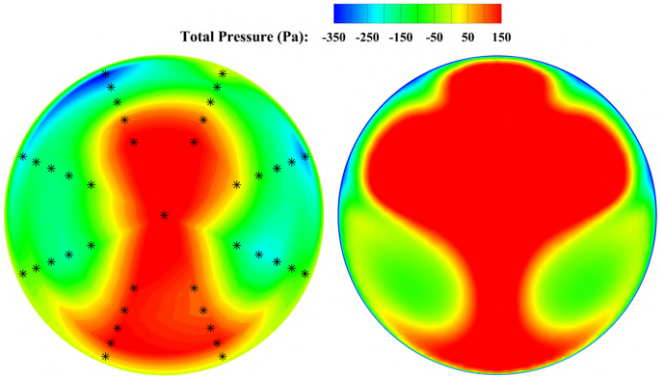

Fig 14. Sample of fan face total pressure comparison (relative to atmospheric pressure) highlighting presence of vortices

4. Conclusion

The work contained in this paper has provided an overview of selected results pertaining to the subsonic aerodynamics, performance, control and stability of a the HEXAFLY-INT vehicle. The focus of this work has been not only presenting static and dynamic derivatives, but understanding the behaviour of the vortex dominated flowfield, and the mechanisms behind the aircraft handling qualities. Results for both the low speed variant and glider configuration have been presented. As little literature on the topic of hypersonic vehicles in the low speed flow regime exists, the data generated at the University of Sydney will provide the groundwork, not only for the HEXAFLY-INT vehicle, but also for future hypersonic aircraft looking to take-off and land horizontally.

References

[1] K. Bowcutt, "Physics Drivers of Hypersonic Vehicle Design," in *22nd AIAA International Space Planes and Hypersonics Systems and Technologies Conference, 17-19 September 2018, Orlando, Florida*, 2018.

[2] S. Candel, "Concorde and the Future of Supersonic Transport," *Journal of Propulsion and Power*, vol. 20, no. 1, pp. 59–68, 2008.

[3] Qantas News Room, "Record-Breaking Direct New York to Sydney Flight Touches Down," 2019. https://www.qantasnewsroom.com.au/media-releases/record-breaking-direct-new-york-to-sydney-flight-touches-down/.

[4] J. Steelant, "Achievements Obtained for Sustained Hypersonic Flight within the LAPCAT project," in *15th AIAA International Space Planes and Hypersonic Systems and Technologies Conference 28 April - 1 May 2008, Dayton, Ohio*, 2008.

[5] J. Steelant, R. Varvill, C. Walton, S. Defoort, K. Hannemann, and M. Marini, "Achievements Obtained for Sustained Hypersonic Flight within the LAPCAT-II project," in *20th AIAA International Space Planes and Hypersonic Systems and Technologies Conference AIAA, 6-9 July 2015, Glasgow, Scotland*, 2015.

[6] G. Pezzella, M. Marini, M. Cicala, A. Vitale, T. Langener, and J. Steelant, "Aerodynamic Characterization of HEXAFLY Scramjet Propelled Hypersonic Vehicle," in *32nd AIAA Applied Aerodynamics Conference 16-20 June 2014 Atlanta, Georgia*, 2014.

[7] C. Meerts and J. Steelant, "Air intake design for the deceleration propulsion unit of the LAPCAT-MR2 hypersonic aircraft," in *5th European Conference for Aerospace Sciences (EUCASS) July 1-5 2013, Munich, Germany*, 2013.

[8] T. Langener, S. Erb, and J. Steelant, "Trajectory simulation and optimization of the LAPCAT-MR2 hypersonic cruiser concept," in *29th Congress of the International Council of the Aeronautical Sciences (ICAS) 7-12 September, 2014 St. Petersburg, Russia*, 2014.

[9] J. Roskam, *Airplane Flight Dynamics and Automatic Flight Controls Part 1*. Lawrence: DARcorportation, 4 ed., 2001.

[10] F. Ferguson, M. Dhanasar, and I. Blankson, "Waverider Design and Analysis," in *20th AIAA International Space Planes and Hypersonic Systems and Technologies Conference Waverider, 6-9 July 2015, Glasgow, Scotland*, 2015.

[11] T. Zhang, Z. Wang, W. Huang, and L. Yan, "Parameterization and optimization of hypersonic-gliding vehicle configurations during conceptual design," *Aerospace Science and Technology*, vol. 58, pp. 225–234, 2016.

[12] L. Chen, X. Deng, Z. Guo, Z. Hou, and W. Wang, "A novel approach for design and analysis of volume-improved osculating-cone waveriders," *Acta Astronautica*, vol. 161, pp. 430–445, 2019.

[13] F. Ding, J. Liu, C. Shen, W. Huang, Z. Liu, and S. Chen, "An overview of waverider design concept in airframe/inlet integration methodology for air-breathing hypersonic vehicles," *Acta Astronautica*, vol. 152, pp. 639–656, 2018.

[14] S. Di Giorgio, D. Quagliarella, G. Pezzella, and S. Pirozzoli, "An aerothermodynamic design optimization framework for hypersonic vehicles," *Aerospace Science and Technology*, vol. 84, no. September, pp. 339–347, 2019.

[15] F. Chen, H. Liu, and S. Zhang, "Time-adaptive loosely coupled analysis on fluid–thermal–structural behaviors of hypersonic wing structures under sustained aeroheating," *Aerospace Science and Technology*, vol. 78, no. July, pp. 620–636, 2018.

[16] P. Roncioni, P. Natale, M. Marini, T. Langener, and J. Steelant, "Numerical simulations and performance assessment of a scramjet powered cruise vehicle at mach 8," *Aerospace Science and Technology*, vol. 42, pp. 218–228, 2015.

[17] F. Ding, J. Liu, C. Shen, Z. Liu, S. Chen, and X. Fu, "An overview of research on waverider design methodology," *Acta Astronautica*, vol. 140, pp. 190–205, 2017.

[18] P. Rodi, "Preliminary Ramjet/Scramjet Integration with Vehicles Using Osculating Flowfield Waverider Forebodies," in *30th AIAA Applied Aerodynamics Conference 25 - 28 June 2012, New Orleans, Louisiana*, 2012.

[19] M. Mirmirani, C. Wu, A. Clark, S. Choi, and R. Colgren, "Modeling for Control of a Generic Airbreathing Hypersonic Vehicle," in *AIAA Guidance, Navigation, and Control Conference and Exhibit 15 - 18 August 2005, San Francisco, California*, 2005.

[20] B. Fidan, M. Mirmirani, and P. Ioannou, "Flight Dynamics and Control of Air-Breathing Hypersonic Vehicles: Review and New Directions," in *12th AIAA International Space Planes and Hypersonic Systems and Technologies 15 - 19 December 2003, Norfolk, Virginia*, 2003.

[21] J. Dickeson, A. Rodriguez, S. Sridharan, J. Benavides, and D. Soloway, "Decentralized Control of an Airbreathing Scramjet-Powered Hypersonic Vehicle," in *AIAA Guidance, Navigation, and Control Conference 10 - 13 August 2009, Chicago, Illinois*, 2009.

[22] X. Liu, W. Liu, and Y. Zhao, "Navier-Stokes predictions of dynamic stability derivatives for air-breathing hypersonic vehicle," *Acta Astronautica*, vol. 118, pp. 262–285, 2016.

[23] D. Hahne, "Evaluation of the Low-Speed Stability and Control Characteristics of a Mach 5.5 Waverider Concept," 1997.

[24] I. Blankson, M. Lewis, and R. Pap, "Subsonic Experiments using the LoFLYTE Hypersonic Waverider Vehicle," in *AIAA 8th International Space Planes and Hypersonic Systems and Technologies Conference, Norfolk, VA*, 1998.

[25] J. Neidhoefer, C. Gibson, R. Saeks, C. Cox, M. Kocher, and L. Hunt, "Accurate Automation Corporation's LoFLYTE Program," in *AIAA's 1st Technical Conference and Workshop on Unmanned Aerospace Vehicles, 20-23 May 2002, Portsmouth, Virginia*, 2002.

[26] R. Miller, B. Argrow, R. Miller, and B. Argrow, "Subsonic aerodynamics of an osculating cones waverider," in *35th AIAA Aerospace Sciences Meeting & Exhibit, 6-9 January, 1997 Reno, Nevada*, 1997.

[27] R. Pap, R. Saeks, C. Lewis, A. Carlton, C. Cox, M. Kocher, and T. Kersting, "The LoFLYTE program," in *33rd Joint Propulsion Conference and Exhibit 6 - 9 July 1997, Seattle, Washington*, 1997.

[28] R. Saeks, C. Cox, and R. Pap, "LoFLYTE - A neurocontrols testbed," in *35th Aerospace Sciences Meeting and Exhibit 6 January - 9 January 1997 Reno, Nevada*, 1997.

[29] C. Lewis, C. Cox, R. Saeks, R. Pap, E. Wagner, and P. Hagseth, "Development of the LoFLYTE Vehicle," in *34th Aerospace Sciences Meeting and Exhibit, 15 - 18 January 1996 Reno, Nevada*, 1996. January.

[30] C. Gibson, R. Vess, and R. Pegg, "Low Speed Flight Testing of a X-43A Hypersonic Lifting Body Configuration," in *12th AIAA International Space Planes and Hypersonic Systems and Technologies 15 - 19 December 2003, Norfolk, Virginia*, 2003.

[31] C. Gibson, J. Neidhoefer, S. Cooper, L. Carlton, C. Cox, and C. Jorgensen, "Development and Flight Test of the X-43A-LS Hypersonic Configuration UAV," in *AIAA's 1st Technical Conference and Workshop on Unmanned Aerospace Vehicles, S 20-23 May 2002, Portsmouth, Virginia*, 2002.

[32] J. Steelant, V. Villace, M. Marini, G. Pezzella, B. Reimann, S. Chernyshev, A. Gubanov, V. Talyzin, N. Voevodenko, N. Kukshinov, A. Prokhorov, A. Neely, C. Kennell, D. Verstraete, and D. Buttsworth, "Numerical and experimental research on aerodynamics of a high-speed passenger vehicle within the HEXAFLY-INT project," *30th Congress of the International Council of the Aeronautical Sciences (ICAS), 25-29 September 2016, Daejeon, Korea*, 2016.

[33] G. Pezzella, M. Marini, B. Reimann, and J. Steelant, "Aerodynamic design analysis of the HEXAFLY-INT hypersonic glider," *20th AIAA International Space Planes and Hypersonic Systems and Technologies Conference 6-9 July 2015, Glasgow, Scotland*, 2015.

[34] T. Bykerk, D. Verstraete, S. Wolf, V. Villace, and J. Steelant, "Performance and stability analysis of a hypersonic vehicle for a low speed flight test program," in *HiSST : International Conference on High-Speed Vehicle Science Technology, 26-29 November 2018, Moscow, Russia*, 2018.

[35] T. Bykerk, D. Verstraete, J. Steelant, V. Fernández-Villacé, and S. Wolf, "Analysis of a modified scramjet intake for a low speed flight test program of a hypersonic waverider," in *ISABE 2019 22 - 27th September, 2019, Canberra, Australia*, 2019.

[36] T. Bykerk, D. Verstraete, G. A. Vio, and J. Jeyaratnam, "Low Speed Aerodynamics and Static Stability of Hypersonic Vehicles," *Australasian Fluid Mechanics Conference*, no. December, pp. 8–11, 2016.

[37] T. Bykerk, D. Verstraete, and J. Steelant, "Low speed longitudinal dynamic stability analysis of a hypersonic waverider using unsteady reynolds averaged navier stokes forced oscillation simulations," *Aerospace Science and Technology*, vol. 103, p. 105883, 2020.

[38] T. Bykerk, D. Verstraete, and J. Steelant, "Low speed lateral-directional dynamic stability analysis of a hypersonic waverider using unsteady reynolds averaged navier stokes forced oscillation simulations," *Aerospace Science and Technology*, vol. 106, p. 106228, 2020.

[39] T. Bykerk, D. Verstraete, and J. Steelant, "Low speed longitudinal aerodynamic , static stability and performance analysis of a hypersonic waverider," *Aerospace Science and Technology*, vol. 96, 2020.

[40] T. Bykerk, D. Verstraete, and J. Steelant, "Low speed lateral-directional aerodynamic and static stability analysis of a hypersonic waverider," *Aerospace Science and Technology*, vol. 98, 2020.

[41] J. Jeyaratnam, T. Bykerk, and D. Verstraete, "Low Speed Stability Analysis of a Hypersonic Vehicle Design Using CFD and Wind Tunnel Testing," in *21st AIAA International Space Planes and Hypersonics Technologies Conference, 6-9 March 2017, Xiamen, China*, 2017.

[42] N. Alemdaroglu, I. Iyigiin, M. Altun, F. Quagliotti, and G. Guglieri, "Measurements of Dynamic Stability Derivatives using Direct Forced Oscillation Technique," in *ICIASF 2001 Record, 19th International Congress on Instrumentation in Aerospace Simulation Facilities, 27-30 August 2001, Cleveland, Ohio*, 2001.

[43] G. Guglieri and F. Quagliotti, "Determination of dynamic stability parameters in a low speed wind tunnel," in *9th Applied Aerodynamics Conference*, (Reston, Virigina), American Institute of Aeronautics and Astronautics, 9 1991.

[44] L. P. Erm, "An Experimental Investigation Into the Feasibility of Measuring Static and Dynamic Aerodynamic Derivatives in the DSTO Water Tunnel," tech. rep., DSTO, 2013.

[45] R. M. Cummings, S. A. Morton, and S. G. Siegel, "Numerical prediction and wind tunnel experiment for a pitching unmanned combat air vehicle," *Aerospace Science and Technology*, vol. 12, no. 5, pp. 355–364, 2008.

[46] G. Hoe, D. Bruce Owens, and C. Denham, "Forced oscillation wind tunnel testing for FASER flight research aircraft," *AIAA Atmospheric Flight Mechanics Conference 2012*, pp. 1–12, 2012.

[47] D. Freeman, "Dynamic Stability Derivatives of Space Shuttle Orbiter Obtained From Wind-Tunnel and Approach and Landing Flight Tests," tech. rep., NASA, 1980.

[48] C. Freeman and P. Boyden, "Subsonic and Transonic Dynamic Stability Characteristics of a Space Shuttle Orbiter," tech. rep., NASA, 1975.

[49] K. Lehmkühler, *A Direct Comparison of Small Aircraft Dynamics between Wind Tunnel and Flight Tests*. PhD thesis, The University of Sydney, 2017.

[50] M. Anderson, *A Methodology for Aerodynamic Parameter Estimation of TailSitting Multi-Rotors*. PhD thesis, The University of Sydney, 2018.